ACS Medicinal Chemistry Letters



Letter

# Radiochemical Synthesis and Evaluation of 13N-Labeled 5-Aminolevulinic Acid for PET Imaging of Gliomas

Adam B Pippin, Ronald J Voll, Yuancheng Li, Hui Mao, and Mark M. Goodman

*ACS Med. Chem. Lett.*, **Just Accepted Manuscript** • DOI: 10.1021/acsmedchemlett.7b00311 • Publication Date (Web): 15 Nov 2017



ACS Publications

ACS Medicinal Chemistry Letters is published by the American Chemical Society. 1155 Sixteenth Street N.W., Washington, DC 20036

# Radiochemical Synthesis and Evaluation of $^{13}$N-Labeled 5-Aminolevulinic Acid for PET Imaging of Gliomas

Adam B. Pippin,*[,1,†,‡] Ronald J. Voll,[1] Yuancheng Li,[1,‡] Hui Wu,[1] Hui Mao,[1,‡] and Mark M. Goodman[1,‡]

[1]Department of Radiology and Imaging Sciences, Emory University Center for Systems Imaging, Wesley Woods Health Center, 1841 Clifton Road, NE, Atlanta, Georgia 30329, United States

*KEYWORDS: 5-ALA, brain tumor, cancer, positron emission tomography, imaging*

**ABSTRACT:** The endogenous amino acid, 5-aminolevulinic acid (5-ALA), has received significant attention as an imaging agent, including on-going clinical trials for image-guided tumor resection due to its selective uptake and subsequent accumulation of the fluorescent protoporphyrin IX in tumor cells. Based on the widely reported selectivity of 5-ALA, a new Positron Emission Tomography imaging probe was developed by reacting methyl 5-bromolevuinate with [$^{13}$N] ammonia. The radiotracer, [$^{13}$N] 5-ALA, was produced in high radiochemical yield (65%) in 10 minutes, and could be purified using only solid phase cartridges. *In vivo* testing in rats bearing intracranial 9L glioblastoma showed peak tumor uptake occurred within 10 minutes of radiotracer administration. Immunohistochemical staining and fluorescent imaging was used to confirm the tumor location and accumulation of the tracer seen from the PET images. The quick synthesis and rapid tumor specific uptake of [$^{13}$N] 5-ALA makes it a potential novel clinical applicable radiotracer for detecting and monitoring tumors non-invasively.

Brain tumors present additional challenges for diagnosis and treatment due to the intracranial location, involvement of the central nervous system and difficult to deliver imaging and therapeutic agents through the blood brain barrier. Gliomas make up 80% of malignant brain tumors and often result in poor prognosis and decreased life expectancy[1]. Diagnosing brain tumors heavily depends on invasive procedures of cranial biopsy or after tumor resection. Current first pass diagnostic imaging for brain tumors[2] such as MRI and CT provide mostly anatomical and morphological details, but lack of molecular and functional information.

The endogenous amino acid, 5-aminolevulinic acid (5-ALA), is the first compound in the biological synthesis of heme in mammals[3]. It is found that enhanced uptake of 5-ALA in cancerous cells provides an accumulation of a fluorescent porphyrin known as Protoporphyrin IX (PpIX)[4]. While the preferential accumulation of 5-ALA in tumors still remains an area of active investigation, the current proposed mechanisms include: increased 5-ALA entry through a disrupted blood brain barrier[5], upregulation of beta[6] and oligopeptide transporters[7] (PEPT1 and PEPT2), increased expressions of enzymes in the heme biosynthesis pathway and decreased amount of the enzyme ferrochetelase[8]. In particular, 5-ALA is useful for brain tumors because of its selective fluorescence in gilomas[9]. It is widely reported that PpIX is preferentially accumulated in glioblastoma cells with ratios of 20 to 50:1 compared to normal brain cells[10,11]. Primary transportation through the blood brain barrier occurs through the choroid plexus[12], however, leaky vascular may also be a factor when tumors are present in the brain[5]. Therefore, there are increasing interests and efforts in developing clinical applications of 5-ALA. For example, 5-ALA and its esters[13] have found use in fluorescence-guided surgery to help visualize tumorous tissue in neurosurgical procedures[11]. The use of 5-ALA as an intraoperative imaging probe for determining tumor margins during the resection of malignant gliomas has been found to increase the rate of gross total resection to 65% compared to 35% without 5-ALA[14]. The progression-free survival rate at 6 months is also increased to 41% when using 5-ALA versus 21% without[14,15]. In addition, 5-ALA shows promise for future therapeutic applications for cancer using photodynamic therapy (PDT). In this therapy technique, the preferential accumulation of PpIX in tumors provides a substrate which when exposed to UV light, results in reactive oxygen species that can ultimately kill cancer cells[16]. While the fluorescence of PpIX can be useful for therapeutic applications, imaging PpIX for diagnostic purposes is limited to superficial tumors or intraoperative procedures due to poor light penetration through the skin[17,18].

Using a radiolabled version of 5-ALA for Positron Emission Tomography (PET) not only can overcome the limitations of optical detectability but also can potentially provide a highly tumor specific PET tracer compared to existing [$^{18}$F] fluorodeoxyglucose (FDG), which often has strong background signals due to the high uptake in brain parenchyma[19]. Furthermore, 5-ALA PET scanning would be useful for pre-operative planning in conjunction to surgical resection procedures that use 5-ALA to visualize tumors for fluorescence-guided surgery. Thus, an amino acid-based PET tracer may be more useful for imaging tumors in the brain[20-23]. Additionally, a 5-ALA based radioligand could also help determine the viability of a candidate for PDT when using 5-ALA as a photosensitizer. There is also evidence that the uptake of 5-ALA is variable in different tumor lines[24,25]. A PET ligand may be used to quantitate the rate of PpIX synthesis[26,27]. This information could potentially be used to non-invasively grade or differentiate brain tumors based on the PpIX metabolism. These wide arrays of potential applications lead us to seek a method to develop a radioactive

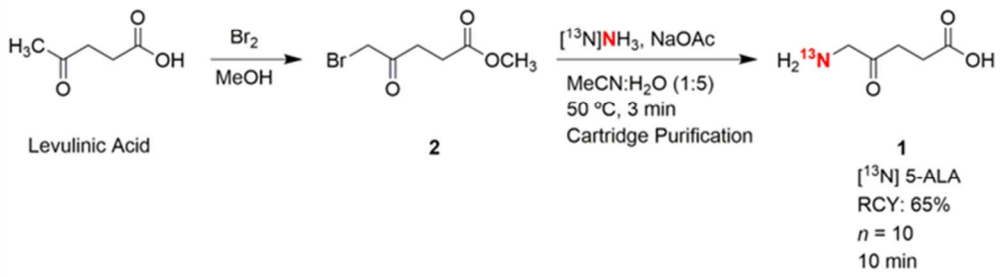


**Scheme 1.** Synthesis of the precursor, methyl 5-bromolevulinate **2**, and radiochemical synthesis of [$^{13}$N] 5-ALA **1**.

version of the naturally occurring amino acid that would be suitable for use with PET imaging.

The molecule 5-ALA lends itself to very few practical installments of a PET radioisotope. Without altering the compound, the only usable PET isotopes are $^{11}$C, $^{13}$N, and $^{15}$O. Ideally, $^{11}$C would be the best-suited isotope due to its extensive use in the field of PET imaging and its longer half-life (20 min). Unfortunately, at this time, there are no facile ways of synthesizing a $^{11}$C version of 5-ALA in high radiochemical yield. To date, only a $^{11}$C derivative of 5-ALA, 5-amino-4-oxo-[6-$^{11}$C]hexanoic acid ([$^{11}$C] MALA) has been synthesized[17]. This novel radiotracer was created by installing a $^{11}$C methyl group on an oxime precursor using tetrabutyl ammonium fluoride and [$^{11}$C] methyl iodide in DMSO. There were several drawbacks to this radiosythesis: the precursor was difficult to purify, the reaction results in a racemic mixture, the synthesis is multiple steps, preparatory HPLC is required, radiochemical yield was low (4.4% uncorrected decay), and the resulting radiotracer is not a natural occurring amino acid. Non-radioactive MALA, was found to be an inhibitor of 5-aminolevulinate dehydratase ($K_i$ = 0.2 M), and thus can only be used to estimate the synthesis rate of PpIX[17,28]. Because of these factors and our previous experience working with the quick decaying $^{13}$N isotope[29], we sought to produce the naturally occurring [$^{13}$N] 5-ALA radiotracer **1**. Herein, we describe the radiochemical synthesis of [$^{13}$N] 5-ALA **1** and demonstrate its use in tumor imaging in a rat model of glioma using the 9L glioma cell line.

The precursor for [$^{13}$N] 5-ALA **1**, methyl 5-bromolevulinate **2**, was synthesized by reacting levulinic acid with bromine in methanol (**Scheme 1**). This reaction has been studied at great length in a variety of different solvents including ionic liquids[30,31]. The reaction of bromine with levulinic acid typically produces a mixture of 3-bromo, 5-bromo, and 3,5-dibromo isomers depending on the solvent used. Using methanol as a solvent, the non-optimized reaction resulted in a 30% yield of the desired isomer after separation using silica column chromatography. The amount of methyl 5-bromolevulinate produced was sufficient for labeling studies.

[$^{13}$N] Ammonia is produced by bombarding water containing ethanol (0.25%) as a reductant[32]. After eluting the cyclotron product through a QMA cartridge to remove residual [$^{18}$F] fluoride, [$^{13}$N] ammonia can be trapped on a CM cartridge in near quantitative recovery. The [$^{13}$N] ammonia can be eluted off the CM cartridge in aqueous form by an increase in ionic strength. In a typical experiment, a 30 minute bombardment (60 μA) produced around 250 mCi (9.25 GBq) of [$^{13}$N] ammonia.

For the production of [$^{13}$N] 5-ALA **1**, the [$^{13}$N] ammonia was eluted off the cartridge with aqueous sodium acetate (1 mL, 3 M) into a vial containing the precursor **2** (8 mg) dissolved in acetonitrile (250 μL) (**Scheme 1**). Heating the vial for 3 minutes at 50 ºC was sufficient for complete radioisotope incorporation, but to ensure no [$^{13}$N] ammonia was present, the vial was purged with argon for 2 minutes to remove any volatile unreacted [$^{13}$N] ammonia. Due to time constraints and the lack of side products, the radiotracer was quickly purified using only cartridges to remove any remaining precursor. The crude reaction mixture was loaded by vacuum onto tC18 and HLB cartridges (Waters) into a waste vial. A small amount of [$^{13}$N] 5-ALA **1** (<20 mCi or 0.74 GBq) was detected in the waste vial but the majority of radioactivity was retained on the two cartridges. Eluting 3 mL of an acidic solution through the Sep-Paks provided the radiotracer [$^{13}$N] 5-ALA **1** in high radiochemical yield (65% decay corrected) (**Scheme 1**). Using acidic phosphate (0.2 M, pH = 5), acetic acid/sodium acetate (0.2 M, pH = 6), or HCl (10 mmol, pH = 2) for elution all provided similar yields (~100 mCi or 3.7 GBq). To ensure no particles were present, the purified solution was pressure filtered through a 0.2 μm filter into a sterile vial and subsequently used immediately in studies. The total time from the end of bombardment to dose was 10 minutes. The dose formulation was intentionally made slightly acidic (pH = 6) to ensure dimerization did not occur. It is well known that when non-radioactive 5-ALA is formulated at neutral or basic pH, it can rapidly dimerize to 2,5-dicarboxyethyl-3,6-dihydropyrazine (DHPY) and further oxidize to produce 2,5-dicarboxyethylpyrazine (PY)[33]. In an acidic formulation, the radiotracer shelf-life was longer than its decay.

Due to the short half-life of $^{13}$N, the quality control on the amino acid was conveniently performed using radio thin layer chromatography. This is the type of analysis routinely used for the quality control of polar radiotracers. For a more in-depth analysis, the polar nature of this amino acid requires the use of hydrophilic interaction chromatography to assay the quality of the dose produced[17]. The 5-ALA HCl salt standard lacks a significant chromophore and requires that low wavelengths (210 nm) be used. This also makes determining specific activity difficult. The only source of ammonia should be from the cyclotron target, we estimate the specific activity of [$^{13}$N] 5-ALA **1** is similar to [$^{13}$N] ammonia (> 2 Ci/μmol or 74 GBq/μmol) for the end of synthesis.

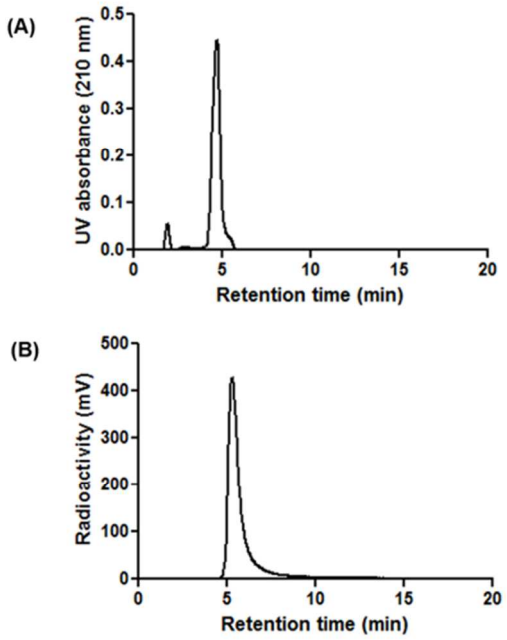


**Figure 1.** HPLC profiles of 5-ALA. (A) UV absorbance (210 nm) of unlabeled 5-ALA. (B) Radioactivity (mV) of [$^{13}$N] 5-ALA.

Studies reported by Hebeda et al showed 5-ALA was readily taken up in 9L glioma cells implanted in rats by using fluorescence to detect PpIX[34]. Therefore, we chose to use the 9L cells to prepare the rat intracranial tumor model to test [$^{13}$N] 5-ALA *in vivo* using microPET imaging. The studies were conducted in male rats with 9L cells surgically implanted into the right hemisphere of the brain. After 12 to 14 days, in which the 9L tumors typically grow to 3-5 mm in size, dynamic PET imaging was performed for 60 minutes followed by a CT scan to obtain the anatomic images.

PET images (**Figure 2**) show that the 9L tumor takes up [$^{13}$N] 5-ALA, resulting in observation of high signal intensity at the tumor region with a signal intensity ratio of 1.5 compared to the symmetrical contralateral normal brain tissue in the left hemisphere (**Figure 3**). Peak uptake of [$^{13}$N] 5-ALA in the tumor cells occurred within 10 minutes. To confirm and validate the imaging results, the animals were sacrificed immediately after the imaging experiments to collect the whole brains and snap frozen before storing in -80 °C. Each brain was then sectioned to 1 mm thick slices for fluorescent imaging using the wavelength of PpIX to determine the distribution in the brain, followed by the H&E staining for tumor region identification. **Figure 4** shows PET, optical images and H&E staining of the brain slice from one of the animals**.** H&E staining indicate the location of the 9L tumor and corresponding PET image which correlates well with the high signal region in the PpIX fluorescent image.

In conclusion, we have successfully synthesized [$^{13}$N] 5-ALA in high radiochemical yield and purity within 10 minutes. The stability of the radiotracer was high for imaging experiments and no dimerization was observed. This rapid synthesis time and lack of HPLC purification makes the radiotracer [$^{13}$N] 5-ALA suitable for additional imaging experiments of other tumor cell lines.

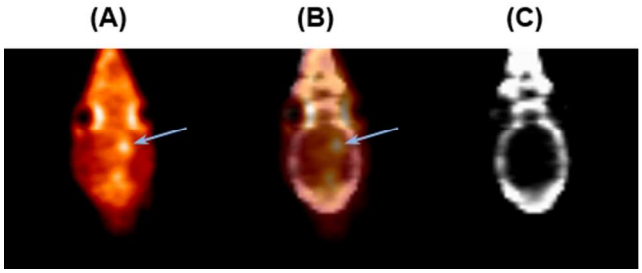


**Figure 2.** Summed coronal PET images (0-15 min) of a rat bearing intracranial 9L glioma: (A) [$^{13}$N] 5-ALA in the brain, (B) coregistered PET-CT, (C) CT template**.** The arrow indicates the location of the tumor.

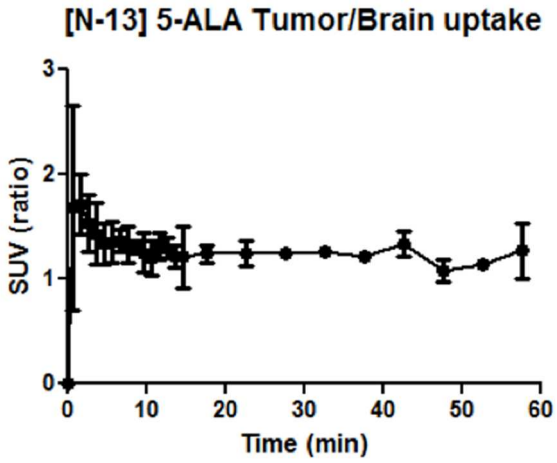


**Figure 3.** Ratio of [$^{13}$N] 5-ALA uptake in the 9L tumor (right hemisphere) vs normal brain tissue (left hemisphere) ($n$ = 3).

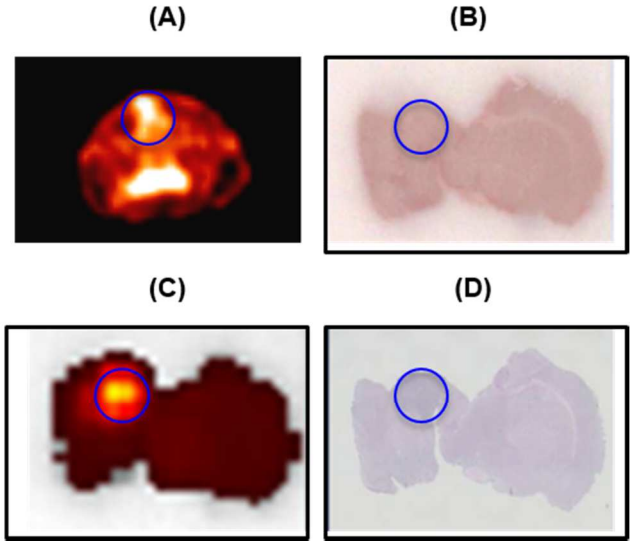


**Figure 4.** (A) Transverse PET summed image (0-15 min) of the brain. (B) Post mortem brain slice. (C) Optical image of the brain slice shown in B. (D) Immunohistochemical (H&E) staining of the brain slice B. The circle indicates the location of the tumor.

## ASSOCIATED CONTENT

### Supporting Information

Supporting information provides full experimental details and characterization data for organic compounds, and radiochemical procedures. This material is available free of charge via the internet at http://pubs.acs.org

## AUTHOR INFORMATION


### Corresponding Author

* Email: Pippin.17@osu.edu

### Present Addresses

†Laboratory for Translational Research in Imaging Pharmaceuticals. The Ohio State University. 1216 Kinnear Rd. Columbus, OH 43212. Email: Pippin.17@osu.edu


### Author Contributions

The manuscript was written through contributions of all authors. / All authors have given approval to the final version of the manuscript. / ‡These authors contributed equally.


### Funding Sources

This research was financially supported with funds from the Emory School of Medicine "Endowed Chair in Imaging Science" for Mark M. Goodman and National Cancer Institute (R01CA169937-04) to Hui Mao.


### Notes

The authors declare no competing financial interest.


## ACKNOWLEDGMENT

We thank Ronald J. Crowe, Karen B. Dolph, and Michael S. Waldrep for assistance with radioisotope production and Margie Jones, Jonathon A. Nye, and Jaekeun Park for assistance with PET-CT imaging experiments.


## ABBREVIATIONS

5-ALA, 5-aminolevulinic acid; PPIX, Protoporphyrin IX; MRI, Magnetic Resonance Imaging; PET, Positron Emission Tomography; CT, Computed Tomography; PEPT1, Peptide Transporter 1; PEPT2, Peptide Transporter 2; PDT, Photodynmaic Therapy; FDG, Fluorodeoxyglucose; MALA, methyl aminolevulinic acid; QMA, Quaternary Methyl Amine; CM, Carboxy Methylate.

## REFERENCES


(1) Goodenberger, M. L.; Jenkins, R. B. Genetics of Adult Glioma. *Cancer Genetics* **2012**, *205* (12), 613–621.

(2) la Fougere, C.; Suchorska, B.; Bartenstein, P.; Kreth, F. W.; Tonn, J. C. Molecular Imaging of Gliomas with PET: Opportunities and Limitations. *Neuro-Oncology* **2011**, *13* (8), 806–819.

(3) Franken, A. C. W.; Lokman, B. C.; Ram, A. F. J.; Punt, P. J.; van den Hondel, C. A. M. J. J.; de Weert, S. Heme Biosynthesis and Its Regulation: Towards Understanding and Improvement of Heme Biosynthesis in Filamentous Fungi. *Appl. Microbiol. Biotechnol.* **2011**, *91* (3), 447–460.

(4) Casas, A.; Batlle, A. M.; Butler, A. R.; Robertson, D.; Brown, E. H.; MacRobert, A.; Riley, P. A. Comparative Effect of ALA Derivatives on Protoporphyrin IX Production in Human and Rat Skin Organ Cultures. *Br. J. Cancer* **1999**, *80* (10), 1525–1532.

(5) Novotny, A.; Stummer, W. 5-Aminolevulinic Acid and the Blood-Brain Barrier–a Review. *Med. Laser Appl.* **2003**, *18*, 36-40.

(6) Rud, E.; Gederaas, O.; Høgset, A.; Berg, K. 5-Aminolevulinic Acid, but Not 5-Aminolevulinic Acid Esters, Is Transported Into Adenocarcinoma Cells by System BETA Transporters. *Photochem. Photobiol.* **2000**, *71* (5), 640–647.

(7) Ocheltree, S. M.; Shen, H.; Hu, Y.; Xiang, J.; Keep, R. F.; Smith, D. E. Role of PEPT2 in the Choroid Plexus Uptake of Glycylsarcosine and 5-Aminolevulinic Acid: Studies in Wild-Type and Null Mice. *Pharm. Res.* **2004**, *21* (9), 1680–1685.

(8) Ohgari, Y.; Nakayasu, Y.; Kitajima, S.; Sawamoto, M.; Mori, H.; Shimokawa, O.; Matsui, H.; Taketani, S. Mechanisms Involved in Aminolevulinic Acid (ALA)-Induced Photosensitivity of Tumor Cells: Relation of Ferrochelatase and Uptake of ALA to the Accumulation of Protoporphyrin. *Biochem. Pharmacol.* **2005**, *71* (1-2), 42–49.

(9) Ma, R.; Watts, C. Selective 5-Aminolevulinic Acid-Induced Protoporphyrin IX Fluorescence in Gliomas. *Acta Neurochirurgica* **2016**, *158*, 1935–1941.

(10) Pichlmeier, U.; Bink, A.; Schackert, G.; Stummer, W.; the ALA Glioma Study Group. Resection and Survival in Glioblastoma Multiforme: an RTOG Recursive Partitioning Analysis of ALA Study Patients. *Neuro-Oncology* **2008**, *10* (6), 1025–1034.

(11) Li, Y.; Rey-Dios, R.; Roberts, D. W.; Valdés, P. A.; Cohen-Gadol, A. A. Intraoperative Fluorescence-Guided Resection of High-Grade Gliomas: a Comparison of the Present Techniques and Evolution of Future Strategies. *World Neurosurgery* **2014**, *82* (1-2), 175–185.

(12) Ennis, S. R.; Novotny, A.; Xiang, J.; Shakui, P.; Masada, T.; Stummer, W.; Smith, D. E.; Keep, R. F. Transport of 5-Aminolevulinic Acid Between Blood and Brain. *Brain Res.* **2003**, *959* (2), 226–234.

(13) Hexyl Aminolevulinate: 5-ALA Hexylester, 5-ALA Hexylesther, Aminolevulinic Acid Hexyl Ester, Hexaminolevulinate, Hexyl 5-Aminolevulinate, P 1206. *Drugs R D* **2006**, *6* (4), 235–238.

(14) Colditz, M. J.; van Leyen, K.; Jeffree, R. L. Aminolevulinic Acid (ALA)–Protoporphyrin IX Fluorescence Guided Tumour Resection. Part 2: Theoretical, Biochemical and Practical Aspects. *Journal of Clinical Neuroscience* **2012**, *19* (12), 1611–1616.

(15) Pirotte, B. J. M.; Levivier, M.; Goldman, S.; Massager, N.; Wikler, D.; Dewitte, O.; Bruneau, M.; Rorive, S.; David, P.; Brotchi, J. Positron Emission Tomography-Guided Volumetric Resection of Supratentorial High-Grade Gliomas: a Survival Anaylsis in 66 Consecutive Patients. *Neurosurgery* **2009**, *64* (3), 471–481.

(16) Wachowska, M. G.; Muchowicz, A.; Firczuk, M. G.; Gabrysiak, M.; Winiarska, M.; Wa czyk, M. G.; Bojarczuk, K.; Golab, J. Aminolevulinic Acid (ALA) as a Prodrug in Photodynamic Therapy of Cancer. *Molecules* **2011**, *16* (12), 4140–4164.

(17) Suzuki, C.; Kato, K.; Tsuji, A. B.; Kikuchi, T.; Zhang, M.-R.; Arano, Y.; Saga, T. Synthesis and in Vitro Celluar Uptake of $^{11}$C-Labeled 5-Aminolevulinic Acid Derivative to Estimate the Induced Celluar Accumulation of Protoporphyrin IX. *Bioorganic & Medicinal Chemistry Letters* **2013**, *23* (16), 4567–4570.

(18) Rodriguez, L.; Batlle, A.; Di Venosa, G.; MacRobert, A. J.; Battah, S.; Daniel, H.; Casas, A. Study of the Mechanisms of Uptake of 5-Aminolevulinic Acid Derivatives by PEPT1 and PEPT2 Transporters as a Tool to Improve Photodynamic Therapy of Tumours. *The International Journal of Biochemistry & Cell Biology* **2006**, *38* (9), 1530–1539.

(19) McConathy, J.; Martarello, L.; Malveaux, E. J.; Camp, V. M.; Simpson, N. E.; Simpson, C. P.; Bowers, G. D.; Olson, J. J.; Goodman, M. M. Radiolabeled Amino Acids for Tumor Imaging with PET: Radiosynthesis and Biological Evaluation of 2-Amino-3-[$^{18}$F]Fluoro-2-Methylpropanoic Acid and 3-[$^{18}$F]Fluoro-2-Methyl-2-

(Methylamino)Propanoic Acid. *J. Med. Chem.* **2002**, *45* (11), 2240–2249.

(20) Kato, T.; Shinoda, J.; Nakayama, N.; Miwa, K.; Okumura, A.; Yano, H.; Yoshimura, S.; Maruyama, T.; Muragaki, Y.; Iwama, T. Metabolic Assessment of Gliomas Using $^{11}$C-Methionine, [$^{18}$F] Fluorodeoxyglucose, and $^{11}$C-Choline Positron-Emission Tomography. *American Journal of Neuroradiology* **2008**, *29* (6), 1176–1182.

(21) Jager, P. L.; Vaalburg, W.; Pruim, J.; de Vries, E. G.; Langen, K. J.; Piers, D. A. Radiolabeled Amino Acids: Basic Aspects and Clinical Applications in Oncology. *J. Nucl. Med.* **2001**, *42* (3), 432–445.

(22) Smits, A.; Baumert, B. G. The Clinical Value of PET with Amino Acid Tracers for Gliomas WHO Grade II. *International Journal of Molecular Imaging* **2011**, *2011* (4), 1–11.

(23) Kaschten, B.; Stevenaert, A.; Sadzot, B.; Deprez, M.; Degueldre, C.; Del Fiore, G.; Luxen, A.; Reznik, M. Preoperative Evaluation of 54 Gliomas by PET with Fluorine-18-Fluorodeoxyglucose and/or Carbon-11-Methionine. *J. Nucl. Med.* **1998**, *39* (5), 778–785.

(24) Krieg, R. C.; Messmann, H.; Rauch, J.; Seeger, S.; Knuechel, R. Metabolic Characterization of Tumor Cell-Pecific Protoporphyrin IX Accumulation After Exposure to 5-Aminolevulinic Acid in Human Colonic Cells. *Photochem. Photobiol.* **2002**, *76* (5), 518–525.

(25) Namikawa, T.; Yatabe, T.; Inoue, K.; Shuin, T.; Hanazaki, K. Clinical Applications of 5-Aminolevulinic Acid-Mediated Fluorescence for Gastric Cancer. *World Journal of Gastroenterology* **2015**, *21* (29), 8769–8775.

(26) Phelps, M. E. *PET: Molecular Imaging and Its Biological Applications*; Springer, 2004.

(27) Carson, R. E.; Herscovitch, P.; Daube-Witherspoon, M. E. *Quantitative Functional Brain Imaging with Positron Emission Tomography*; Academic Press: San Diego, 1998.

(28) Erskine, P. T.; Newbold, R.; Brindley, A. A.; Wood, S. P.; Shoolingin-Jordan, P. M.; Warren, M. J.; Cooper, J. B. The X-Ray Structure of Yeast 5-Aminolaevulinic Acid Dehydratase Complexed with Substrate and Three Inhibitors. *Journal of Molecular Biology* **2001**, *312* (1), 133–141.

(29) Pippin, A. B.; Mohd Arshad, Z. H.; Voll, R. J.; Nye, J. A.; Ghassabian, S.; Williams, C. M.; Mancini, A.; Liotta, D. C.; Smith, M. T.; Goodman, M. M. In Vitro Metabolic Stability and in Vivo Biodistribution of 3-Methyl-4-Furoxancarbaldehyde Using PET Imaging in Rats. *ACS Med. Chem. Lett.* **2016**, *7* (6), 563–567.

(30) MacDonald, S. F. Methyl 5-Bromolevulinate. *Canadian Journal of Chemistry* **1974**, *52*, 3257–3258.

(31) Zavozin, A. G.; Kravchenko, N. E.; Ignat ev, N. V.; Zlotin, S. G. Variation in the Regioselectivity of Levulinic Acid Bromination in Ionic Liquids. *Tetrahedron Letters* **2010**, *51* (3), 545–547.

(32) Gómez-Vallejo, V.; Gaja, V.; Gona, K. B.; Llop, J. Nitrogen-13: Historical Review and Future Perspectives. *J. Label Compd. Radiopharm.* **2014**, *57* (4), 244–254.

(33) Bunke, A.; Zerbe, O.; Schmid, H.; Burmeister, G.; Merkle, H. P.; Gander, B. Degradation Mechanism and Stability of 5-Aminolevulinic Acid. *J. Pharm. Sci.* **2000**, *89* (10), 1335–1341.

(34) Hebeda, K. M.; Saarnak, A. E.; Olivo, M.; Sterenborg, H. J.; Wolbers, J. G. 5-Aminolevulinic Acid Induced Endogenous Porphyrin Fluorescence in 9L and C6 Brain Tumours and in the Normal Rat Brain. *Acta Neurochir. (Wien)* **1998**, *140* (5), 503–513.

Insert Table of Contents artwork here

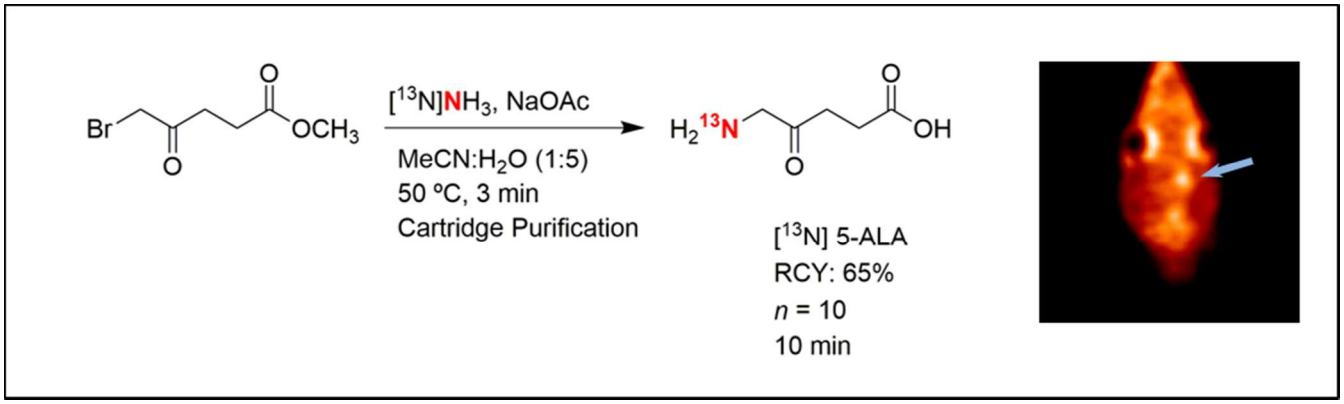

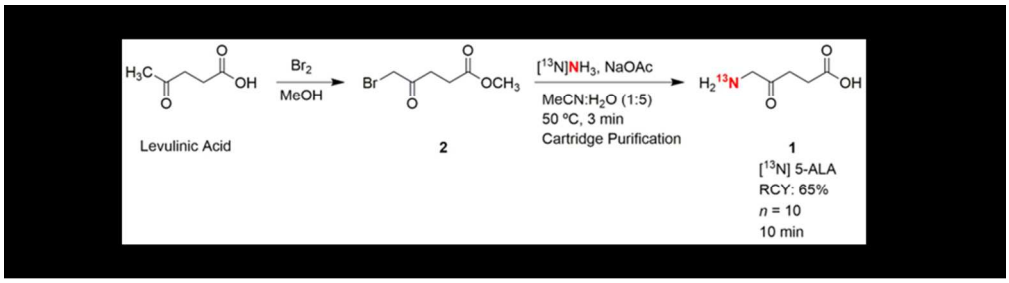


Scheme 1. Synthesis of the precursor, methyl 5-bromolevulinate 2, and radiochemical synthesis of [13N] 5-ALA 1.

177x48mm (150 x 150 DPI)

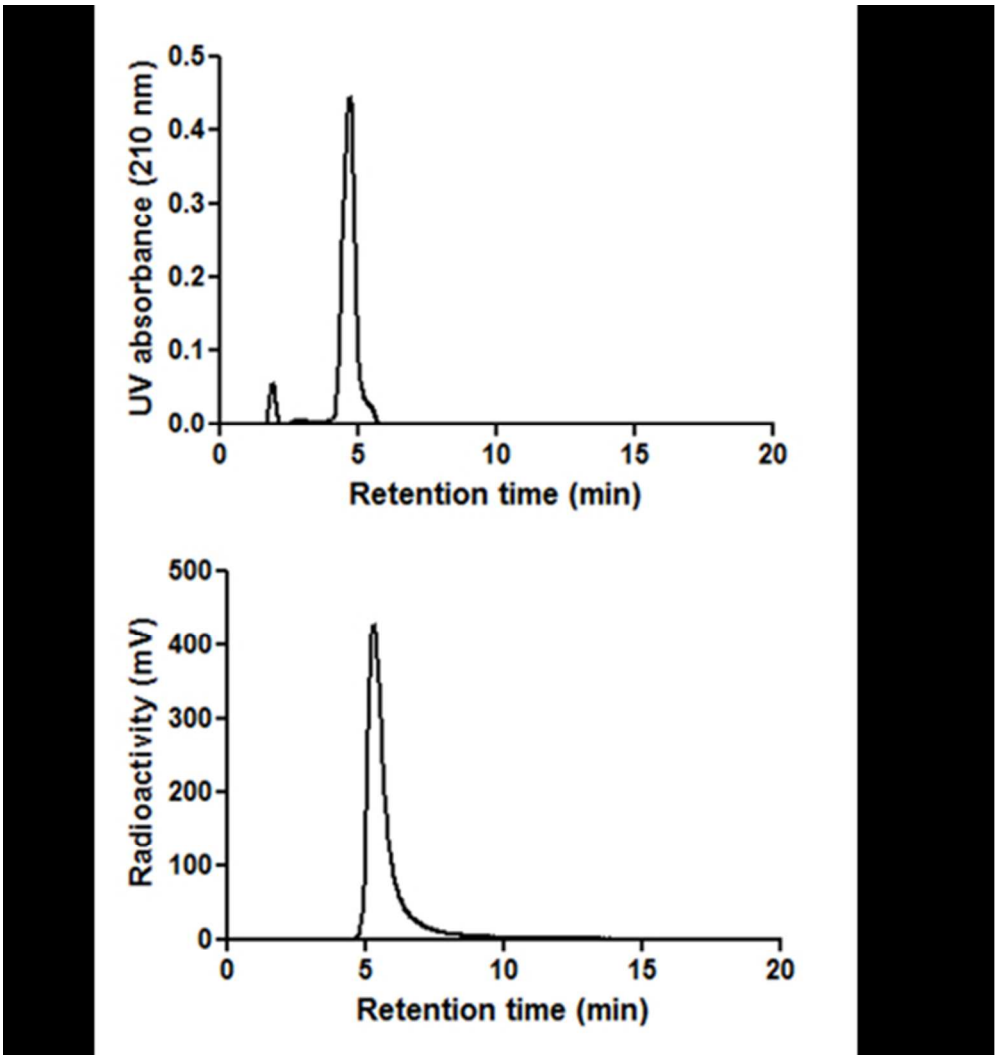


Figure 1. HPLC profiles of 5-ALA. (A) UV absorbance (210 nm) of unlabeled 5-ALA. (B) Radioactivity (mV) of [13N] 5-ALA.

83x88mm (150 x 150 DPI)

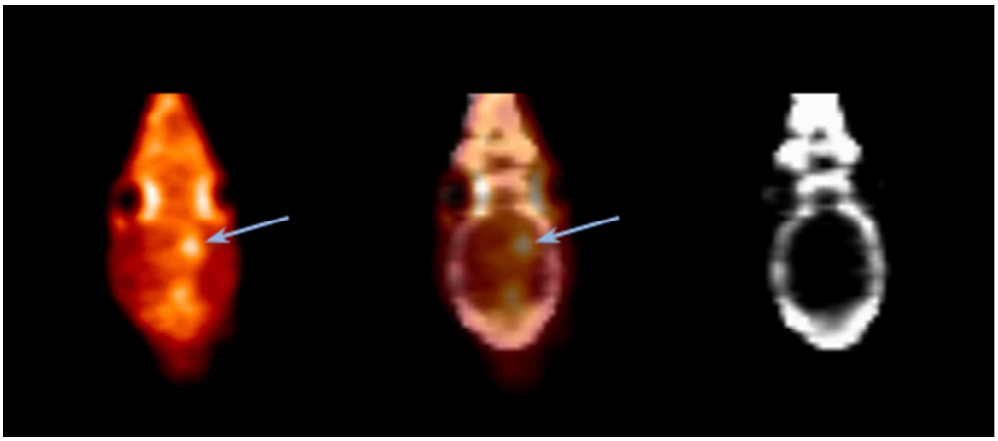

Figure 2. Summed coronal PET images (0-15 min) of a rat bearing intracranial 9L glioma (arrow): (A) [13N] 5-ALA in the brain, (B) coregistered PET-CT, (C) CT template.

83x36mm (150 x 150 DPI)

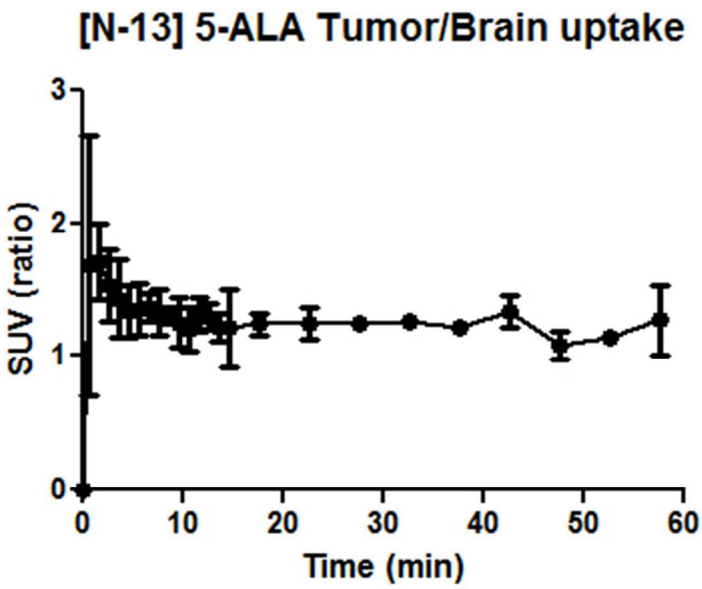


Figure 3. Ratio of [13N] 5-ALA uptake in the 9L tumor (right hemisphere) vs normal brain tissue (left hemisphere) (n = 3).

83x66mm (122 x 122 DPI)

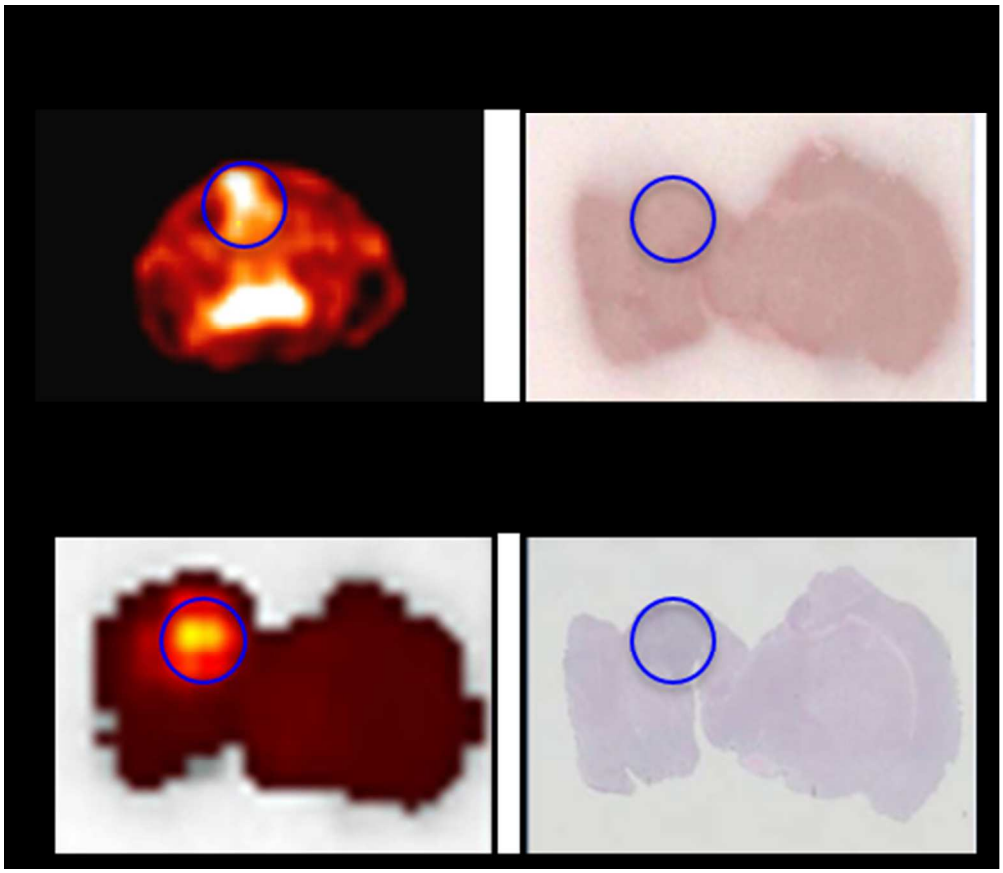

Figure 4. (A) Transverse PET summed image (0-15 min) of the brain. (B) Post mortem brain slice. (C) Optical image of the brain slice shown in B. (D) Immunohistochemical (H&E) staining of the brain slice B.

84x72mm (150 x 150 DPI)

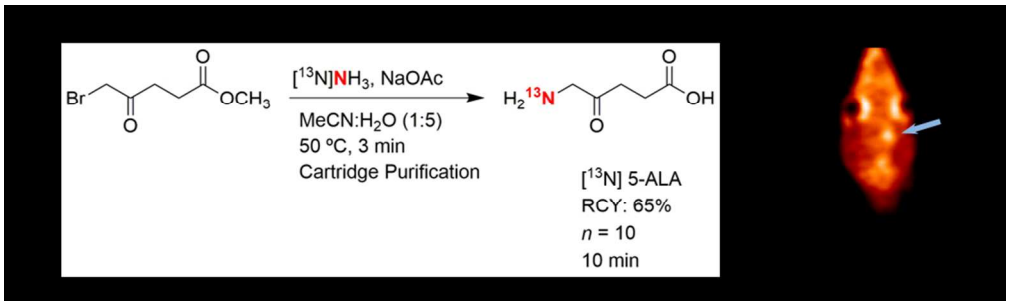


Table of contents graphic

182x53mm (150 x 150 DPI)